JOURNAL OF COMPUTATIONAL PHYSICS 17, 68–78 (1975)

Use of the Spectral Method for Two- and Three-Dimensional Guiding Center Plasmas

YEHUDA SALU AND GEORG KNORR

Department of Physics and Astronomy, University of Iowa, Iowa City, Iowa 52242

Received June 7, 1974; revised September 19, 1974

The spectral method is shortly reviewed and then applied to equations of two- and three-dimensional guiding center plasmas. Some linear and nonlinear phenomena have been studied. It is shown that the spectral method can be used on a wide range of problems.

I. INTRODUCTION

The solution of three-dimensional plasma problems imposes severe demands on computer time and/or core memory. If N points are sufficient in one dimension (1D), roughly N^3 points should be used in 3D. In addition, the number of variables, equations, and their complexity increases with more dimensions. It is therefore important to choose an economical representation of the solutions of the partial differential equations.

We can represent a solution on a mesh or by the coefficients of a set of orthogonal functions. We assume that the function to be represented is "smooth," i.e., has n continuous derivatives, $n \geqslant 1$. Then it follows that any of the N points on a grid must be in the neighborhood of the adjacent points. On the other hand, the coefficients of the orthogonal functions can be choosen independently of each other, except that for large order the coefficients have to tend to zero. It thus appears that N coefficients of orthogonal functions convey more information than N points on a grid.

For our case the natural choice is Fourier modes. An additional advantage is that derivatives and integrals of any order can be calculated "exactly" for a given representation. For nonlinear problems products have to be calculated. In Fourier space this corresponds to convolution sums. Transforming from Fourier space into configuration space and performing the multiplication there turns out to be faster than evaluating the convolution sum. When transforming back into Fourier space, aliasing has to be taken into account. Recent developments, the fast Fourier

transform (FFT) [1] and dealiasing procedures [2, 3] make it competitive with the difference methods under certain conditions.

In the first section we describe in detail the basic features and techniques of the spectral method. In the second section we illustrate the method by dealing with linear, quasilinear, and nonlinear effects occurring in 2D and 3D guiding center plasmas. In the last section we discuss some problems which can be solved by this method.

II. The Spectral Method

Let a set of grid points be defined by

$$X_j = 2\pi j/N, \tag{1}$$

where $j = 0, 1, N-1$, and N is an integer power of 2. Let Z_j be the value of the function $Z(X)$ at X_j, $Z_j = Z(X_j)$. Then the discrete Fourier transform is

$$Z_j = \sum_{|k| \leqslant N/2} z(k) \exp(ikX_j) \qquad (j = 0, 1, \ldots, N-1), \tag{2}$$

and the inverse transform is given by

$$z(k) = 1/N \sum_{j=0}^{N-1} Z_j \exp(-ikX_j) \qquad (|k| \leqslant 1/2N). \tag{3}$$

Differentiating we get

$$\frac{dZ_j}{dX} = \sum_{|k| \leqslant N/2} ikz(k) \exp(ikX_j). \tag{4}$$

This relation is used whenever spacial differentiation is involved.

Assume the set of partial differential equations to be given by

$$(d/dt)\,\mathbf{F}(\mathbf{X}) = \mathbf{G}[\mathbf{F}(\mathbf{X}), t], \tag{5}$$

where $\mathbf{G}$ is a differential operator in the space coordinates. The functions $\mathbf{F}(\mathbf{X})$ are bounded and periodic in the volume L^3. The general solution can then be written as

$$\mathbf{F}(\mathbf{X}, t) = \sum_{-\infty < |m| < \infty} \mathbf{f}_m(t) \exp(i\mathbf{k}_m \cdot \mathbf{X}), \qquad \mathbf{k}_m = \frac{2\pi}{L} \cdot (m_1, m_2, m_3) \quad m_1, m_2, m_3 = 0, \pm 1, \ldots . \tag{6}$$

In the spectral method we assume that there is a finite N for which

$$\tilde{\mathbf{F}}(\mathbf{X}, t) = \sum_{|m|<N/2} \check{\mathbf{f}}_m(t) \exp(i\mathbf{k}_m \cdot \mathbf{X}) \tag{7}$$

is a good approximation to $\mathbf{F}(\mathbf{X})$ of Eq. (6). Using the discrete Fourier transform (2) and (3), all spacial differentiations are done by using (4).

At this point we would like to compare the discrete with the continuous Fourier transforms. The orthogonality condition of the continuous case is

$$\frac{1}{L}\int_0^L \exp[i(k_n - k_m)\, X]\, dX = \delta_{nm}\,, \tag{8}$$

where δ_{nm} is the Dirac delta function. The orthogonality condition for the discrete case is

$$\sum_{j=0}^{N-1} \exp[i(k_n - k_m)\, X_j] = N\delta_{n,m\pm\alpha N}\,, \qquad \alpha = 0, 1, 2, \ldots\,. \tag{9}$$

We obtain, for the continuous case,

$$a_n = \frac{1}{L}\int_0^L \exp(-ik_n X)\, F(X_j)\, dX. \tag{10}$$

a_n is the exact amplitude of the nth Fourier mode. For the discrete case we get

$$b_n = \frac{1}{N}\sum_{j=0}^{N-1} \exp(-ik_n X_j) \cdot F(X_j), \tag{11}$$

where, as a result of the difference between the right sides of Eqs. (8) and (9), we find

$$b_n = a_n + \sum_{\substack{\alpha=-\infty \\ \alpha\neq 0}}^{\infty} a_{n+\alpha N}\,. \tag{12}$$

The sum in the right-hand side of (12) is called the "aliasing term." When aliasing terms appear in the Fourier representation, $ik \cdot b(k)$ is no longer the amplitude of the derivative of the kth mode of $F(X)$. Inserting Eq. (4) into Eq. (5) without taking into account the aliasing terms often results (but not always) in numerical instability, the so called "aliasing instability." The basic assumptions of the spectral method, Eqs. (7) and (4), can only be fulfilled as long as the aliasing term is zero or is explicitly removed from the calculated amplitude.

If aliasing terms are not present at the initial steps of the calculation, they may appear later on due to nonlinear terms. For example, let

$$U_j = \sum_{|n|\leqslant N/2} U(k_n) \exp(ik_n X_j),$$
$$V_j = \sum_{|n|\leqslant N/2} V(k_n) \exp(ik_n X_j) \qquad j = 0, 1, \ldots, N-1. \tag{13}$$

We assume that U_j and V_j do not contain aliasing terms; however the product

$$Z_j = U_j V_j \tag{14}$$

contains modes in the range $|n| \leqslant N$, and aliasing terms might falsify the Fourier amplitudes of Z.

A. *Eliminating Aliasing in a One-Dimensional Case*

If we want to represent K Fourier modes of a solution of a nonlinear differential equation, it should be represented on a $4K$ mesh instead of on the minimal $2K$ mesh. Then the product $Z = U \cdot V$ of (13) and (14) is represented on this mesh in a way that its $2K$ modes have the exact nonaliased amplitudes. At this step all $z(k)$ for which $|k_n| > 2K$ should be replaced by zero. Thus these modes will not alias the quantities U and V later on. This method can be used for more dimensions, but there are more economic ways to do it.

B. *Eliminating Aliasing in Many Dimensions*

In the following we give some results obtained by Orszag and Patterson [2, 3]. For further details the reader is referred to the references.

Let

$$U(\mathbf{J}) = \sum_{\|k\|<K} U(\mathbf{k}) \exp[i\mathbf{k} \cdot \mathbf{X}(\mathbf{j})],$$
$$V(\mathbf{J}) = \sum_{\|k\|<K} V(k) \exp[i\mathbf{k} \cdot \mathbf{X}(\mathbf{j})], \tag{15}$$

where $K = N/2$, $\mathbf{X} = (\pi/K)(j_1, j_2, j_3)$, and $j_l = 0, 1, \ldots, N-1$, $l = 1, 2, 3$.

We assume that the only $\mathbf{k}$'s in Eq. (15) for which the amplitude does not vanish are those with

$$k_1^2 + k_2^2 + k_3^2 < (8/9)\, K^2. \tag{16}$$

All other modes are eliminated. Using these $U(k)$ and $V(k)$, we calculate U and V at a shifted grid

$$\mathbf{X}_s = (\pi/K)(j_1 + \tfrac{1}{2}, j_2 + \tfrac{1}{2}, j_3 + \tfrac{1}{2}), \tag{17}$$

and we get

$$U_s(\mathbf{J}) = \sum_{\|k\|<K} U(\mathbf{k}) \exp[i\mathbf{k} \cdot X_s(\mathbf{j})],$$
$$V_s(\mathbf{J}) = \sum_{\|k\|<K} V(\mathbf{k}) \exp[i\mathbf{k} \cdot X_s(\mathbf{j})]. \tag{18}$$

We calculate the products

$$Z(J) = U(J) \cdot V(J),$$
$$Z_s(J) = U_s(J) \cdot V_s(J). \tag{19}$$

Then we Fourier transform the products, using Eq. (3), and obtain the amplitude $z(\mathbf{k})$ and $z_s(k)$, respectively.

Compute

$$\bar{z}(\mathbf{k}) = \tfrac{1}{2}[z(\mathbf{k}) + \exp(-i\mathbf{k} \cdot \mathbf{e}/N) \cdot z_s(k)], \tag{20}$$

(where $\mathbf{e} = (1, 1, 1)$) and eliminate all modes for which (16) does not hold. Then these $\bar{z}(\mathbf{k})$ are the desired nonaliased Fourier modes of the product $Z = U \cdot V$.

This dealiasing procedure is somewhat lengthy; however, it enables us to use the spectral method which is very economical in computer core. Thus we can easily solve three-dimensional problems. This will be demonstrated in the following section.

III. Application to Guiding Center Plasmas

In this section we solve some problems of 2D and 3D guiding center plasma using the spectral method. Some results are new and some are already known and have been included here to illustrate the method. The 3D equations of an electrostatic guiding center plasma are

$$\begin{aligned}
\partial n_i/\partial t &= -\boldsymbol{\alpha} \cdot \nabla n_i - (\partial/\partial Z)(V_i n_i), \\
\partial n_e/\partial t &= -\boldsymbol{\alpha} \cdot \nabla n_e - (\partial/\partial Z)(V_e n_e), \\
\partial V_i/\partial t &= -\boldsymbol{\alpha} \cdot \nabla n_i - V_i(\partial/\partial Z)\, V_i + (e/m_i)\, E_Z\,, \\
\partial V_e/\partial t &= -\boldsymbol{\alpha} \cdot \nabla V_e - V_e(\partial/\partial Z)\, V_e - (1/m_e n_e)(\partial P_e/\partial Z) - (e/m_e)\, E_Z\,, \\
-\nabla^2 \varphi &= (n_i - n_e) \cdot 4\pi l, \\
\boldsymbol{\alpha} &= c(\mathbf{E} \times \mathbf{B})/B^2, \qquad E = -\nabla\varphi.
\end{aligned} \tag{21}$$

Here n_i, n_e, V_i, and V_e are the densities and the average velocities in the Z direction of the ions and electrons, respectively. The direction of the uniform magnetic field B is along the Z axis. m_i and m_e are the ion and electron masses, and P_e is the electron pressure. Equations (21) are the familiar two-fluids equations where the velocities perpendicular to **B** have been replaced by the drift velocity α. The ions are assumed to be cold. Further details about these equations and the assumptions behind them may be found elsewhere [4]. We assume periodic boundary conditions in all directions.

For the 2D case these equations reduce to

$$\begin{aligned} (\partial \Gamma/\partial t) + \alpha \cdot \nabla \Gamma &= 0, \\ -\nabla^2 \varphi &= \Gamma, \end{aligned} \tag{22}$$

where $\Gamma = n_i - n_e$. The 2D equations are equivalent to the 2D hydrodynamic equations of an inviscid incompressible fluid which have been the object of intensive investigations for a long time [5].

The initial values of n_i, n_e, v_i, v_e of Eqs. (21) are specified on an $N \times N \times N$ grid, where N is an integer power of 2. To calculate spatial derivatives we transform from the mesh to k space and employ Eq. (4).

Products (like $V_i n_i$ or $\alpha \nabla n_i$) have to be computed using the dealiasing procedure described in Section II. This way the right-hand sides of the first four equations of system (21) are calculated.

Poisson's equation in (21) is also solved with the aid of the FFT and periodic boundary conditions. The transformed potential is then given by

$$\varphi_{\mathbf{k}} = (n_i - n_e)_{\mathbf{k}} / |\mathbf{k}|^2.$$

The chosen boundary conditions are the most convenient ones for our method. Other conditions (e.g. $\varphi = 0$ at metal walls) can also be incorporated but require further analysis. The algorithm to integrate the first four equations of (21) consists of a second-order predictor–corrector scheme to advance the system in time:

$$\begin{aligned} \mathbf{F}^{n+1/2}(\mathbf{X}) &= \mathbf{F}^n(\mathbf{X}) + \tfrac{1}{2}\Delta t \cdot \mathbf{G}[\mathbf{F}^n(\mathbf{X})], \\ \mathbf{F}^{n+1}(\mathbf{X}) &= \mathbf{F}^n(\mathbf{X}) + \mathbf{G}[\mathbf{F}^{n+1/2}(\mathbf{X})], \end{aligned} \tag{23}$$

where **F** and **G** are defined by Eqs. (5) and (21), and n labels the time step. We repeat that the difference scheme is in time only because the spatial dependence in (21) has already been taken care of by the spectral method.

The two-dimensional algorithm for Eq. (22) is similar (and simpler) than the one described above.

A. *Results of Computer Experiments*

1. *2D Linear and Quasilinear Phenomena*

We first apply the spectral method to study the stability of 2D nonhomogeneous plasma. As a stationary solution we take $\Gamma_0 = \cos(k_0 x)$ and perturb it by $\Gamma_1 = \delta \cos(k_y y)$. Some results for different k_0, k_y, and δ values are plotted in Fig. 1, which shows the time evolution of the energy of mode Γ_1. We see clearly

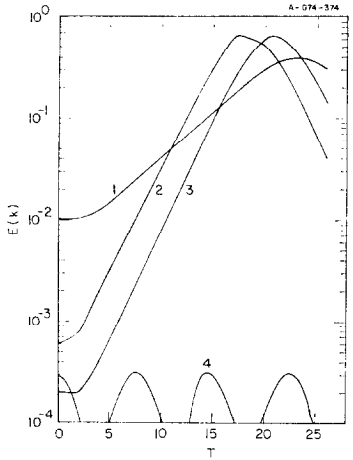

FIG. 1. The energy of the perturbation as a function of time for four experiments. The initial states were:

$$\Gamma_1 = \cos 5x + 0.02 \cos y;\ \Gamma_2 = \cos 5x + 0.02 \cos 4y;$$
$$\Gamma_3 = \cos 5x + 0.01 \cos 4y;\ \Gamma_4 = \cos 4y + 0.02 \cos 5x.$$

that for $K_0 = 4$, $k_y = 5$ we have a stable case, while the other cases are unstable. The numerical growth rates were found to be in good agreement with those obtained from Shoucri [6].

Figure 2 shows how the linear instability is saturated by nonlinear mode coupling. For $9 < T < 15$ the steady state amplitude of mode (5, 0) begins to decay, while the growth rate of modes (0, 4) and (5, 4) is not changed. This we call the quasilinear regime. The results were obtained by taking different length scales in the x and y directions on a 4×4 grid. $\Delta t = 1$.

2. *3D Linear and Quasilinear Phenomena*

We now apply the spectral method to a 3D inhomogeneous plasma. The stationary state $\Gamma_0 = \cos(k_0 x)$ is perturbed by $\Gamma_1 = \delta \cos(k_y y + k_z z)$. The

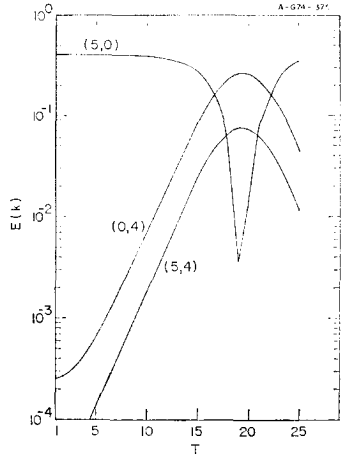

FIG. 2. The energy of the modes (5, 0), (0, 4), and (5, 4) as a function of time for the initial conditions $\Gamma = \cos 5x + 0.02 \sin 4y$.

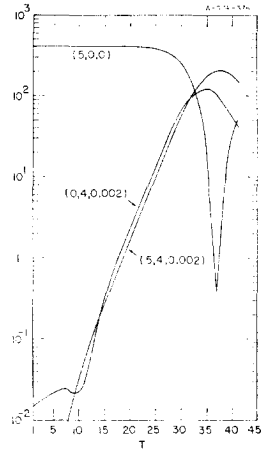

FIG. 3. The energy of the modes (5, 0, 0), (0, 4, 0.002), and (5, 4, 0.002) as a function of time for the initial conditions $N_i = 20 + \cos 5x + 0.02 \cos (4y + 0.002z)$.

results are shown in Fig. 3. Here $\delta = 0.02$, $k_0 = 5$, $k_y = 4$, $k_z = 0.002$, and $m_e/m_i = 2000$.

The linear, quasilinear, and nonlinear stages are similar to those of the 2D case described above. The linear growth rate of the mode $k_x = 5$, $k_y = 4$, $k_z = 0.002$ is 0.15. In this experiment a $4 \times 4 \times 4$ mesh was used. $\Delta t = 1$.

3. *2D Nonlinear Phenomena*

The 2D systems of Eq. (22) have the property that initially present vortices tend to coalesce by nonlinear interactions. Thus the final state often consists of fewer vortices than the initial state [7, 8, 9]. This effect is demonstrated in Fig. 4. A system with ten vortices for $t = 0$ develops to a state of only two main vortices. This run used a 16×16 mesh.

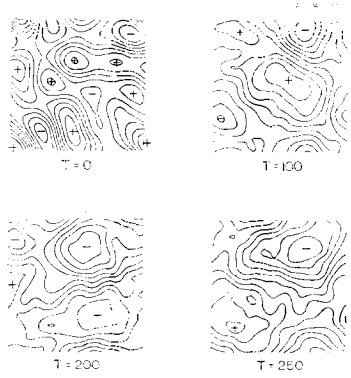

FIG. 4. Equipotentials (or stream lines) for four different times. Vortices marked (+) circulate in opposite sense to those marked (−). It is seen that larger vortices are created in time. Here T = number of time steps, $\Delta t = 0.1$.

B. *Checking the Code*

In the 2D case there are two invariants: the total energy and the vorticity. The energy is given by

$$\sum_K W_K(K) = c_1 = \text{const}, \tag{24}$$

where

$$W_K(K) = \sum_{|\nu|=K} |\Gamma_\nu|^2$$

and the vorticity by

$$\sum_K W_K(K) \cdot K^2 = c_2 = \text{const}. \tag{25}$$

These two quantities were conserved up to the fifth significant digit for sufficiently small time steps ($\Delta t \approx 0.05$).

Another check, which is very simple and applicable to any spectral solution,

is generation of eigenmodes and following their propagation. Linearizing Eq. (22) and taking

$$\begin{aligned} N_i(\mathbf{r}) &= N_{i0} + \delta N_i \cos(\mathbf{k}\cdot\mathbf{r}), \\ N_e(\mathbf{r}) &= N_{e0} + \delta N_e \cos(\mathbf{k}\cdot\mathbf{r}), \\ V_i(\mathbf{r}) &= \delta V_i \cos(\mathbf{k}\cdot\mathbf{r}), \\ V_e(\mathbf{r}) &= \delta V_e \cos(\mathbf{k}\cdot\mathbf{r}), \end{aligned} \tag{26}$$

where $N_{i0} = N_{e0} = N = \text{const}$, we get the known dispersion relation.

$$k_x^2 + k_y^2 + k_z^2 = (k_z^2 N/\omega^2) + [\beta^{-1} k_z^2 N/(\omega^2 - \beta^{-1} k_z^2)], \tag{27}$$

where $\beta^{-1} = m_i/m_e$. For each $\mathbf{k}$ there are two frequencies (corresponding to plasma and ion sound waves). By chosing

$$\begin{aligned} \delta N_i &= \delta N_i, \\ \delta V_i &= \omega\, \delta N_i/k_z N, \\ \delta N_e &= \delta N_i - \omega(k_x^2 + k_y^2 + k_z^2)\, \delta V_i/k_z, \\ \delta V_e &= \delta N_i \left(1 - \frac{\omega^2 k^2}{N k_z^2} - \frac{\omega^2}{k_z^2}\right) \frac{\beta^{-1} k_z}{\omega}, \end{aligned}$$

we have the initial conditions that generate oscillations with only one frequency ω, i.e., we generated an eigenmode. It is very easy to compare the oscillation in that system with the calculated ω, and a good agreement was obtained.

IV. Summary and Conclusions

We have seen how the spectral method is used to solve 2D and 3D plasma problems. This method, which is basically a many-modes interaction calculation, is based on representing the modes by their values at grid points rather than dealing explicitly with their amplitudes and phases. In many cases the "physics of the problem" is contained in a relatively small number of modes. This can sometimes make the spectral method more economical than difference schemes. However, this point has to be checked for each problem separately. The spectral method is especially effective for linear and linearized problems, and for any problem with rapidly converging Fourier series. It appears that problems with discontinuities cannot be economically treated by the spectral method. The dealiasing method can be extended to interaction terms more complicated than the product of two functions.

ACKNOWLEDGMENTS

The authors would like to thank Mr. Magdi Shoucri for communicating his results to us prior to their publication.

This work was supported in part by the Atomic Energy Commission under Grant AT(11-1)-2059.

REFERENCES

1. G. D. BERGLAND, *IEEE Spectrum* July (1969), 41 (This paper includes a detailed list of references on different topics of Fourier transforms and their applications).
2. STEVEN A. ORSZAG, *Studies in Applied Math.* **50** (1971), 293.
3. G. S. PATTERSON, JR. AND STEVEN A. ORSZAG, *Phys. Fluids* **14** (1971), 2538.
4. G. KNORR, Univ. of Iowa Research Report 74-23, submitted to *Phys. Fluids.*
5. P. G. DRAZIN AND L. N. HOWARD, *Advan. Appl. Mech.* **9** (1966), 1.
6. M. SHOUCRI, private communication (The growth rates have been calculated using both a difference scheme and analytical methods where applicable, Ph.D. thesis, University of Iowa, Iowa City, 1974.
7. GLENN JOYCE AND DAVID MONTGOMERY, *J. Plasma Phys.* **10** (1973), 107.
8. N. J. ZABUSKY AND G. S. DEEM, *Fluid Mech.* **47** (1971), 353.
9. F. P. CHRISTIANSEN AND R. S. PECKOVER, United Kingdom Atomic Energy Authority, Research Report CLM-R125, Culham Laboratory, 1973.